WIFAI 2025

11-14 novembre 2025, Bari

Fermilab Muon g-2 final result

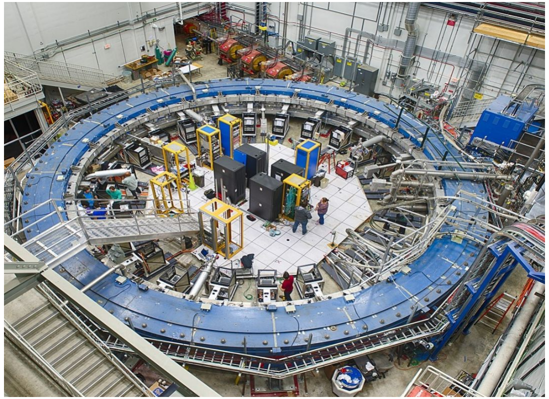

Antonio Gioiosa
Università degli Studi del Molise, INFN
for the FNAL Muon g-2 collaboration

INFN Istituto Nazionale di Fisica Nucleare

Fermilab

μ g-2

Muon g-2 Collaboration

176 collaborators, 34 institutes, 7 countries

Particle-, Nuclear-, Atomic-, Optical-, Accelerator-,and Theoretical-Physicists and Engineers

PRL publication dated 2 Sep 2025

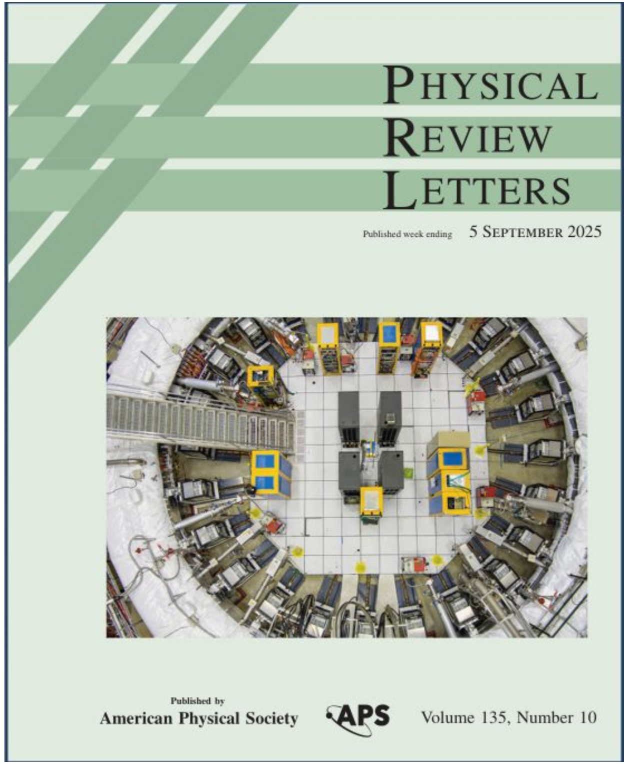

04/09/2025, 13:35 Physical Review Letters - Volume 135 Issue 10

HIGHLIGHTED ARTICLES

FEATURED IN PHYSICS EDITORS' SUGGESTION

Measurement of the Positive Muon Anomalous Magnetic Moment to 127 ppb

D. P. Aguillard *et al.* (Muon $g-2$ Collaboration)

Phys. Rev. Lett. **135**, 101802 (2025) - Published 2 September, 2025

The final results from the Muon $g-2$ experiment agree with the latest predictions of muon's magnetic properties—letting down hopes that the particle would upset the standard model's applecart.

PRL 135 (2025) 101802

Data sample over 6 years (analyzed positrons)

- April 2021: Run-1
- August 2023: Run-2/3 (and combination with Run-1)
- June 2025: Run-4/5/6 (and combination with Run-1/2/3)
- this presentation: Run-4/5/6 analysis and combination with previous results

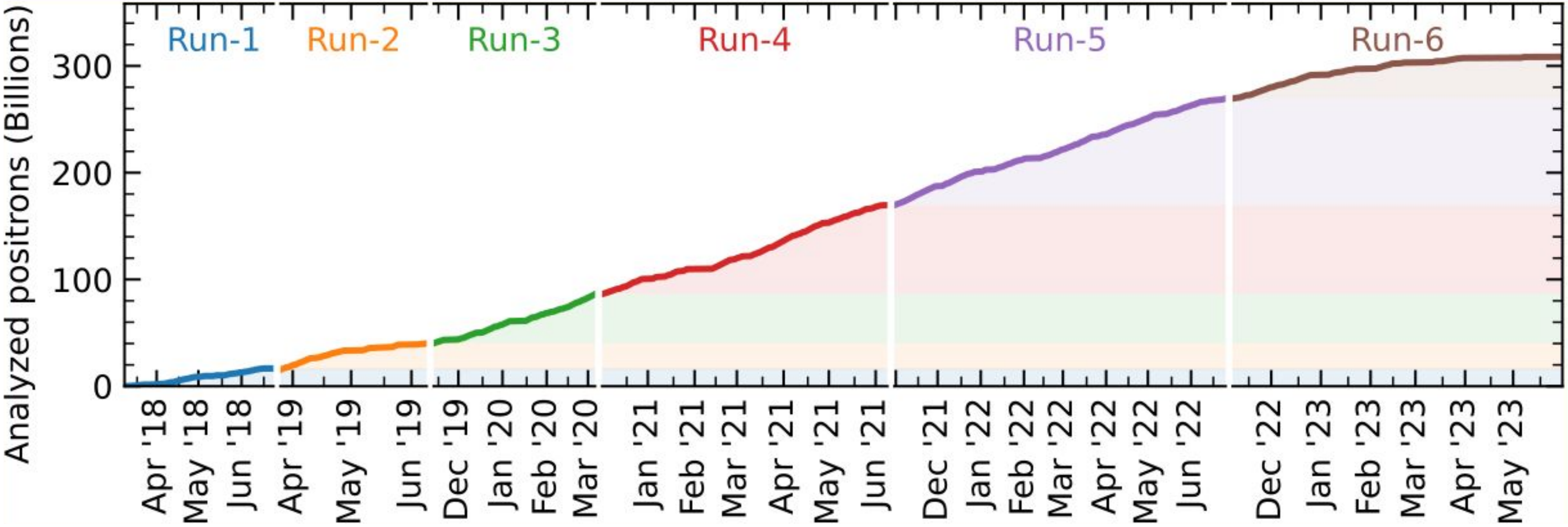

FNAL accelerator complex for Muon g −2

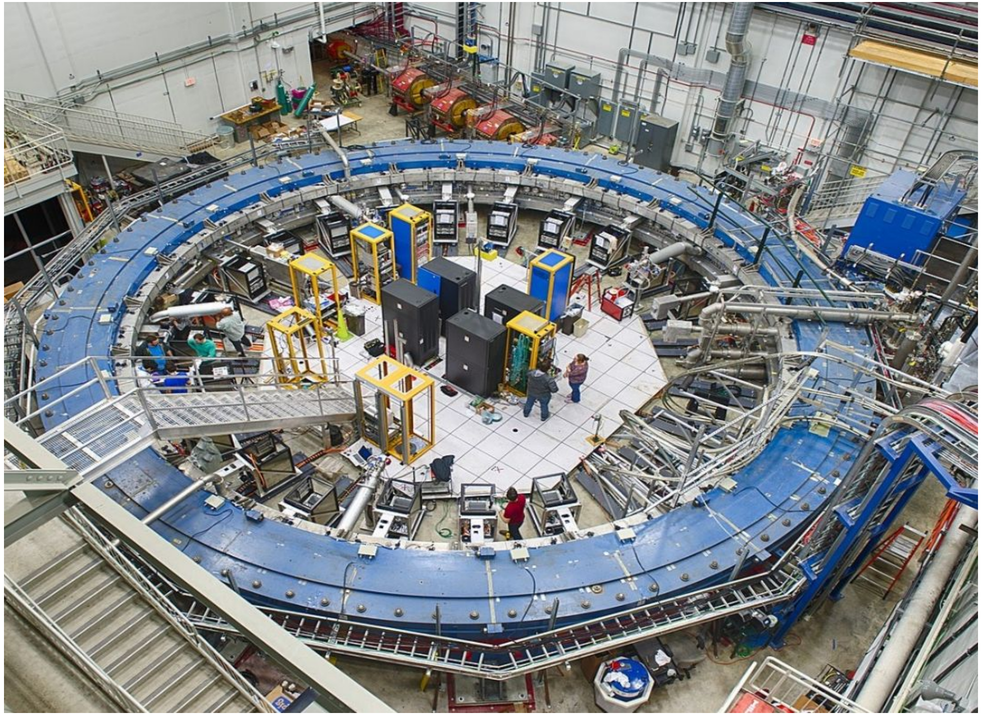

Production of polarized muons

- Dump 8 GeV protons on target to produce pions
- Select pions with momentum $p \simeq 3.11$ GeV
- Let them decay into muons
- In pion rest frame, parity violation in pion decay causes μ^+ spin anti-aligned to momentum vector
- In laboratory frame, highest energy muons are > 90% polarized
- with 8 GeV protons on target, μ^+ are produced more frequently than μ^-

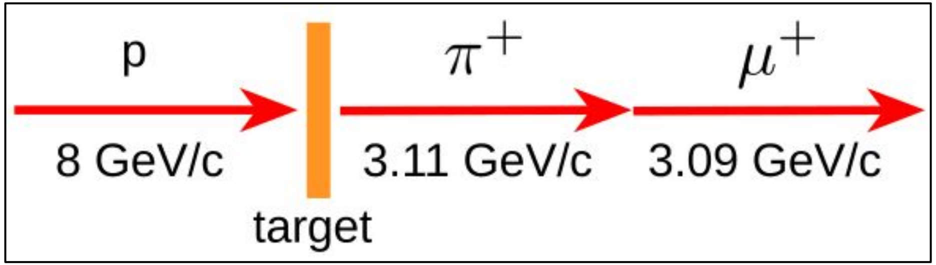

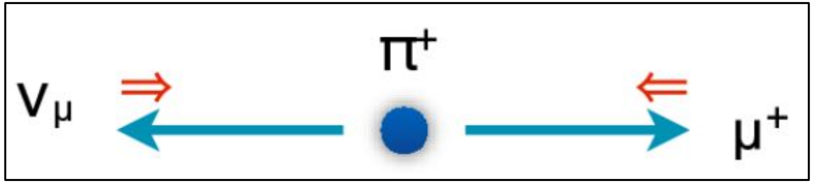

Muon g-2 measurement technique

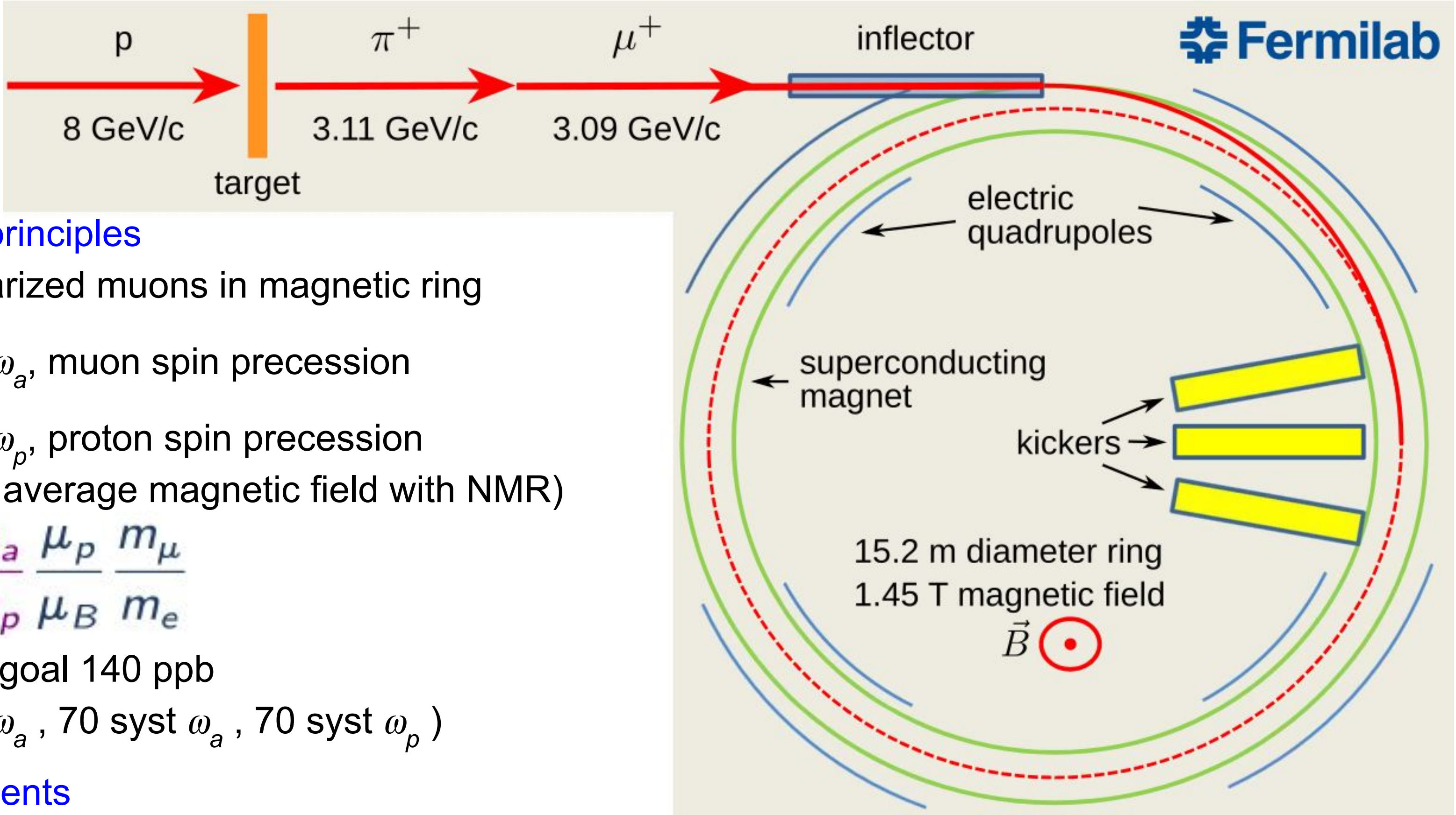

Measurement principles

- Store polarized muons in magnetic ring
- Measure ω_a, muon spin precession
- Measure ω_p, proton spin precession (measure average magnetic field with NMR)
- $$a_\mu = \frac{\omega_a}{\omega_p}\frac{\mu_p}{\mu_B}\frac{m_\mu}{m_e}$$
- Precision goal 140 ppb
- (100 stat ω_a , 70 syst ω_a , 70 syst ω_p)

Main improvements

- More and more pure muons than BNL

Muon g-2 measurement technique, additional details

- Accounting for vertical-focusing electric field and vertical muon beam oscillations:

$$\vec{\omega}_a \equiv \vec{\omega}_s - \vec{\omega}_c = \frac{e}{m_\mu c}\left[a_\mu \vec{B} - \left(a_\mu - \left[\frac{m_\mu c}{p}\right]^2\right)\vec{\beta}\times\vec{E} - a_\mu \frac{(\gamma)}{(\gamma+1)}(\vec{\beta}\cdot\vec{B})\vec{\beta}\right]$$

- zero $\vec{\beta}\times\vec{E}$ term $\Rightarrow$ $p_{\text{magic}} = \frac{m_\mu c}{\sqrt{a_\mu}} \approx$ 3.094 GeV/c Lorentz $\gamma_{\text{magic}} \approx$ 29.3

- muon spin precession $\omega_s \approx g_\mu \frac{eB}{2m_\mu c} + (1-\gamma)\frac{eB}{\gamma m_\mu c}$ $\approx 2\pi \cdot$ 6.9 MHz

  muon cyclotron $\omega_c \approx \frac{eB}{\gamma m_\mu c}$ $\approx 2\pi \cdot$ 6.7 MHz

  muon anomalous precession $\omega_a \approx a_\mu \frac{eB}{m_\mu c}$ $\approx 2\pi \cdot$ 229 kHz

  proton spin precession $\omega'_p(T) \approx g'_p(T)\frac{eB}{2m_p c}$ $\approx 2\pi \cdot$ 61.8 MHz

- ω_a independent (not directly dependent) of uncertainty on muon momentum
- ~5000 stored muons per fill, 12 Hz fills
- ~500 high-energy positrons detected per fill
- ~310 billion analyzed high-energy positrons from muon-decays

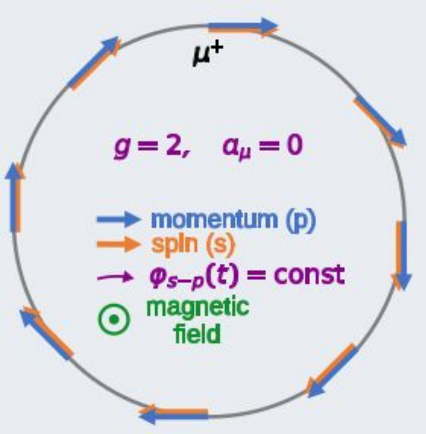

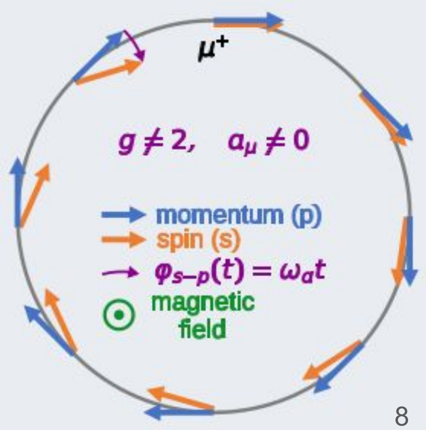

Rate of high-energy muon-decay positrons modulated with cos $\omega_a t$

- Because of parity violation in muon decay, decay positrons peak along muon spin
- Positrons decaying along muon momentum have highest energy in laboratory frame
- $N_e(E_e > E_t) = N_{e0} e^{-t/\tau_\mu}(1 + A \cos \omega_a t)$

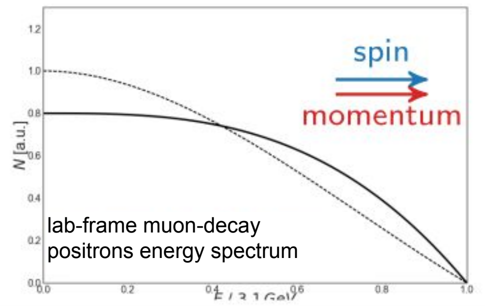

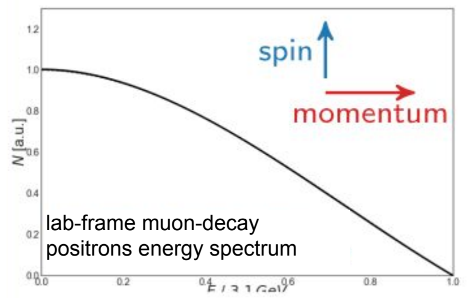

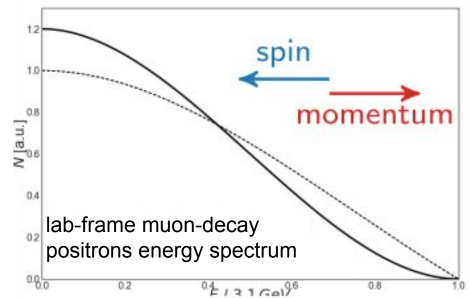

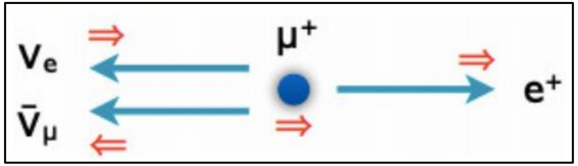

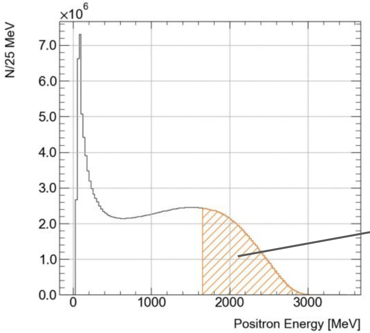

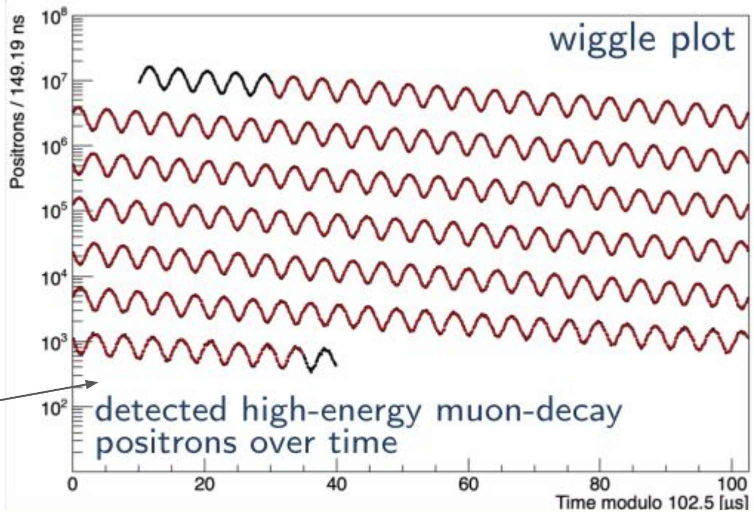

Positrons from positive-muons' decays are detected

- Positrons from positive muons decays curl inward and are detected
- Calorimeters measure energy for ω_a measurement
- Trackers reconstruct muon decay vertices to measure beam dynamics

Each calorimeter module has

- 6×9 PbF_2 crystals array
- 2.5 cm×2.5 cm×14 cm, 15 X_0
- Readout Cherenkov light at 800 MHz with SiPMs
- Continuous gain monitoring with laser system pulses

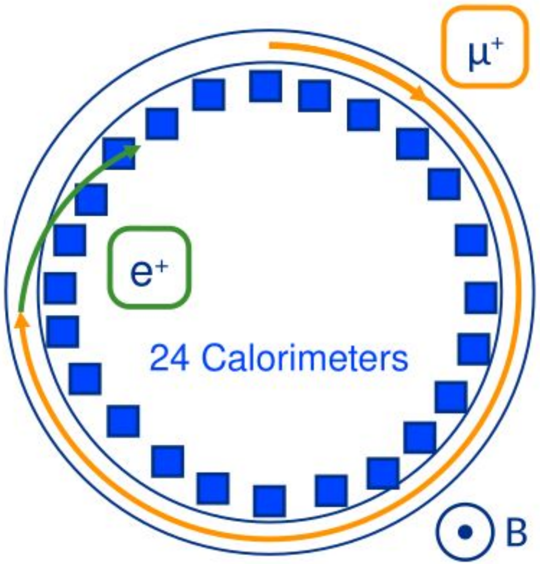

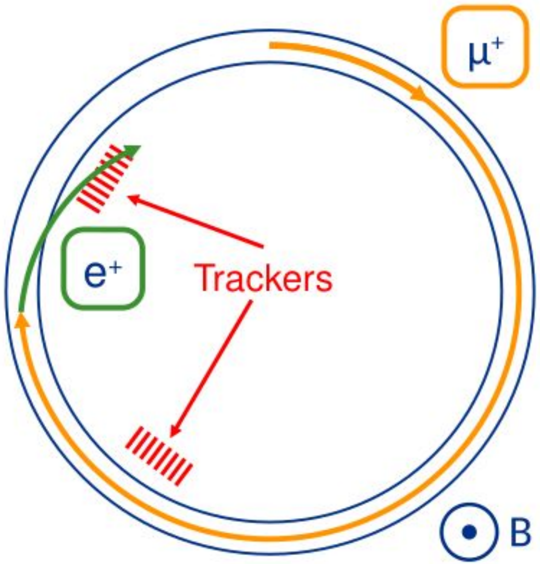

each tracker has

- 8 modules
- 128 straw chambers each
- Trace back muon decay points

Laser calorimeter gain monitoring system

- SiPM gain is reduced by occurrence of preceding hits
- If unaccounted,there is a significant bias on ω_a measurement
- Gain monitored by reading back reference laser light pulses injected in calorimeter crystals
  - Also during data-taking
- Positron energy measurement from SiPM readout corrected for average measured gain loss

SiPM power supply recovery time (μs)

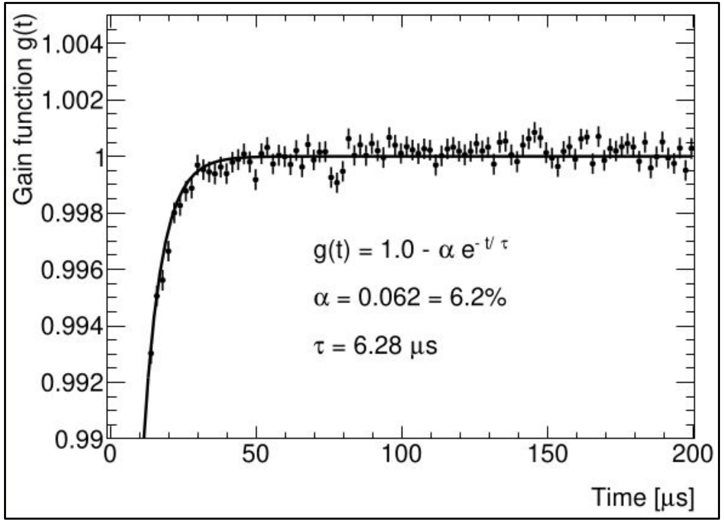

SiPM pixel recovery time (ns)

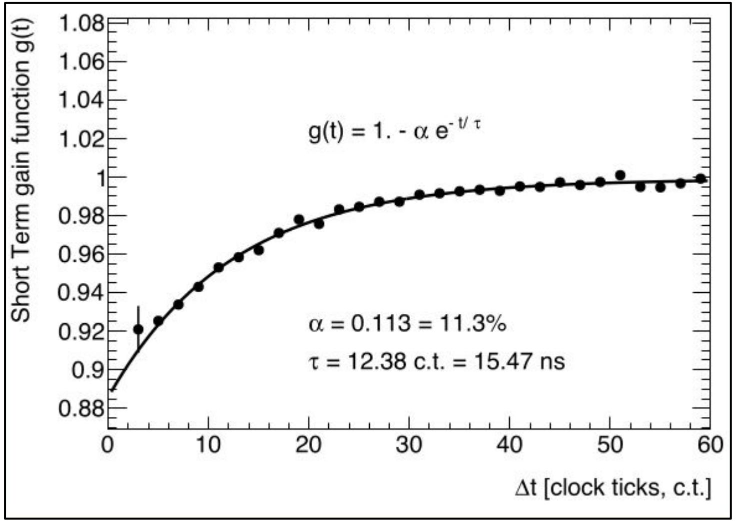

ω_a^m wiggle plot fit, 5 parameters function

$$N(t) = N_0 e^{-t/\tau_\mu}[1 + A\cos(\omega_a t + \varphi)]$$

- $N(t)$: number of e^+ vs. time
- τ_μ: dilated μ^+ life time
- A: Wiggle asimmetry
- ω_a: anomalous precession frequency
- φ: average spin phase at injection

- Peaks in Fourier transform of fit residuals
- Biases of order 1 ppm

Wiggle plot

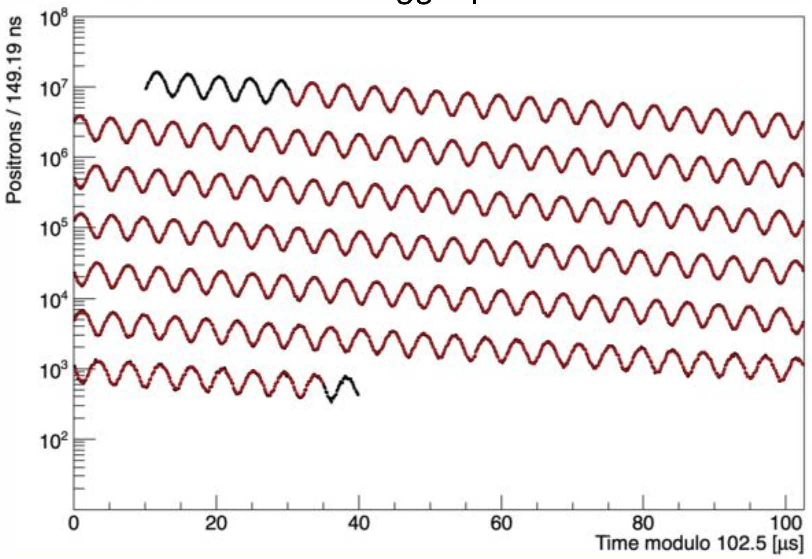

Fourier transform of wiggle plot fit residuals

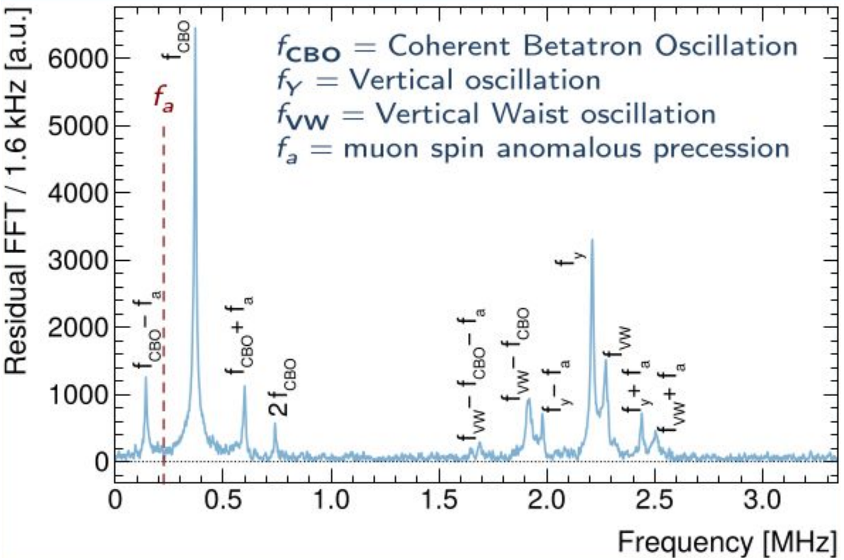

ω_a wiggle plot fit, full function

- ~30-parameter typical fit function to account for
    - Beam vertical and horizontal/radial motion
    - Muon loss
- No peaks in Fourier transform of fit residuals
- Good □^{2} [largest statistics dataset □^{2} / ndof = 4007 / 4097, p = 84%]

Example full ω_a fit function

$$N_0 e^{-\frac{t}{\gamma\tau}} (1 + A \cdot A_{BO}(t) \cos(\omega_a t + \phi \cdot \phi_{BO}(t))) \cdot N_{CBO}(t) \cdot N_{VW}(t) \cdot N_y(t) \cdot N_{2CBO}(t) \cdot J(t)$$

$$A_{BO}(t) = 1 + A_A \cos(\omega_{CBO}(t) + \phi_A) e^{-\frac{t}{\tau_{CBO}}}$$

$$\phi_{BO}(t) = 1 + A_\phi \cos(\omega_{CBO}(t) + \phi_\phi) e^{-\frac{t}{\tau_{CBO}}}$$

$$N_{CBO}(t) = 1 + A_{CBO} \cos(\omega_{CBO}(t) + \phi_{CBO}) e^{-\frac{t}{\tau_{CBO}}}$$

$$N_{2CBO}(t) = 1 + A_{2CBO} \cos(2\omega_{CBO}(t) + \phi_{2CBO}) e^{-\frac{t}{2\tau_{CBO}}}$$

$$N_{VW}(t) = 1 + A_{VW} \cos(\omega_{VW}(t) t + \phi_{VW}) e^{-\frac{t}{\tau_{VW}}}$$

$$N_y(t) = 1 + A_y \cos(\omega_y(t) t + \phi_y) e^{-\frac{t}{\tau_y}}$$

$$J(t) = 1 - k_{LM} \int_{t_0}^{t} \Lambda(t) dt$$

$$\omega_{CBO}(t) = \omega_0 t + A e^{-\frac{t}{\tau_A}} + B e^{-\frac{t}{\tau_B}}$$

$$\omega_y(t) = F \omega_{CBO(t)} \sqrt{2\omega_c / F \omega_{CBO}(t) - 1}$$

$$\omega_{VW}(t) = \omega_c - 2\omega_y(t)$$

Fourier transform of wiggle plot fit residuals

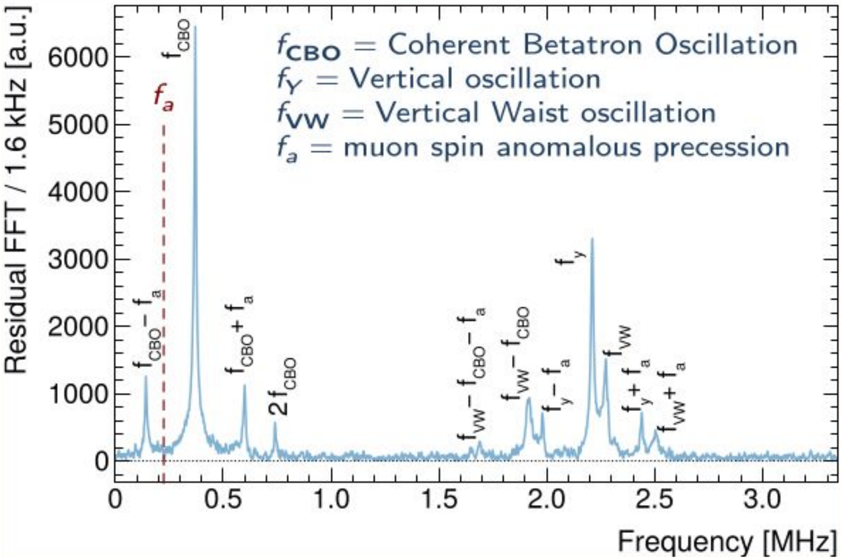

RF on quad HV to dampen radial & vertical beam dynamics

New on Run 4/5/6

- ~1 KV radio-frequency modulation of quad high voltage in first 6 μs of quad activation during fills
- Obtained significant reduction of radial and vertical motion of average muon distribution
- ~10× ω_a bias reduction when not accounting for beam dynamics

Four datasets with different RF damping

- NoRF - no RF
- xRF - RF for radial (x) beam motion
- xyRF5 - RF for radial & vertical beam motion, Run 5
- xyRF6 - RF for radial & vertical beam motion, Run 6

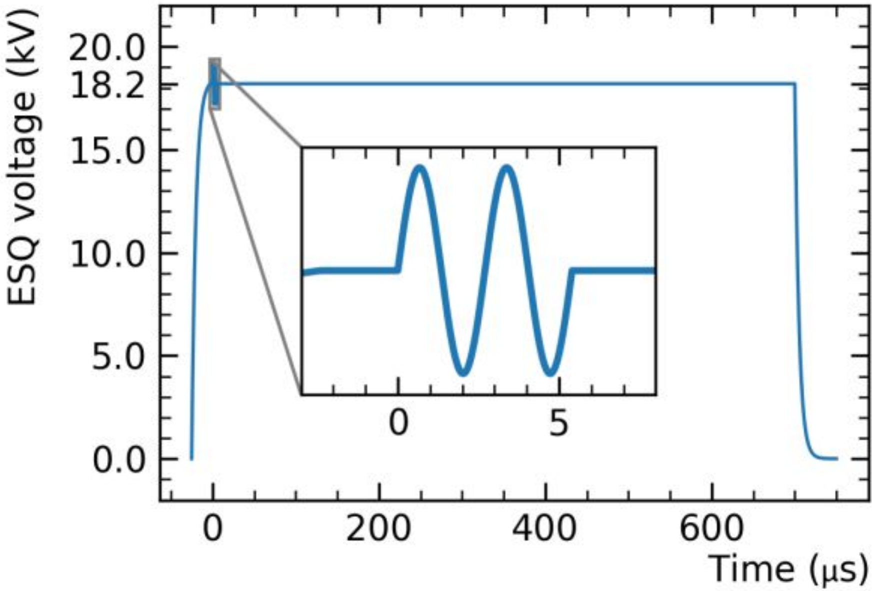

Measuring ω_a^m with ~30 ppb systematic accuracy for Run 4/5/6

- 5 independent and mutually software-blinded analysis groups
- Completed total of 20 analyses (on each of 4 Run 4/5/6 datasets)
- Consistency checks of SW and HW blind analyses
- Consistency checks of common-HW-blinded analyses
- To estimate statistical correlations between analyses
  - Assembled 200 bootstrap samples extracting datasets subruns
  - Estimated between-analyses correlations on data
  - Bootstrap samples planned and performed for most analyses
    (has been done in few cases also when performing Run 2/3 measurement)
- Perform one analysis fit on the wiggle plot assembled for another analysis
- All these tests either succeeded or facilitated debugging and well-understood fixes

New on Run 4/5/6

ω_a^m measurement done separately on 4 datasets

For each dataset, ω_a^m = even average of 7 analyses using most precise methods

- Conservative 100% correlation assumed for each statistical and systematic uncertainty component
- Safe, stable, and only 1.5% larger uncertainty than optimal average

Positron-rate-dependent calorimeter gain sag

New on
Run 4/5/6

- Calorimeter gain sag after calorimeter hits due to SIPM power supply recovery time
  - Well known, measured with laser monitoring system using high power test laser pulses
  - Occurs with injection beam flash, measured with laser monitoring during data-taking, and corrected
- Time-dependent rate of positron hits contributes additional gain sag over fill time
  - Below sensitivity of laser monitoring system during data-taking
  - Dedicated studies estimated order 40 ppb ω_a bias because of phase difference w.r.t. ω_a phase
  - Confirmed with extra studies performed with laser pulses after end of data-taking
- Run 4/5/6: estimated positron gain sag bias subtracted, updated systematic uncertainty
- Run 1 & 2/3: revised published results, accounting for updated understanding

Measurement of the magnetic field map $\omega_p'(T_r)^m$

In-vacuum trolley with NMR probes maps magnetic field every ~3 days

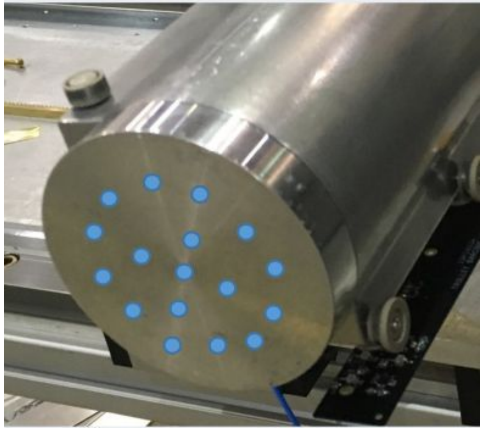
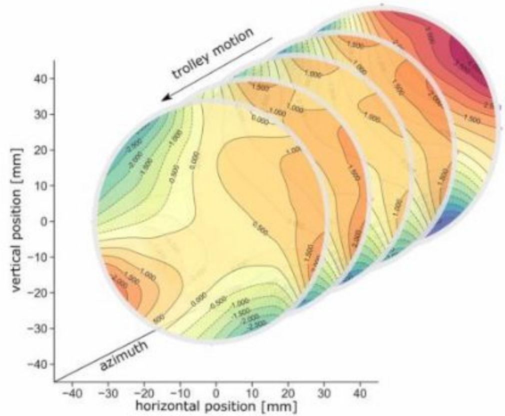

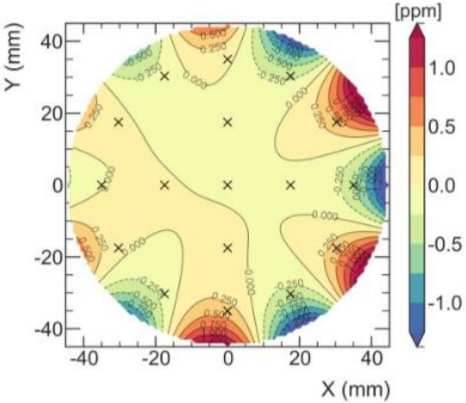

trolley with 17 probes 2-D field maps (~8000 points) azimuthally averaged field map

378 fixed probes monitor field during muon storage at 72 locations

Fixed probes above/below muon storage region


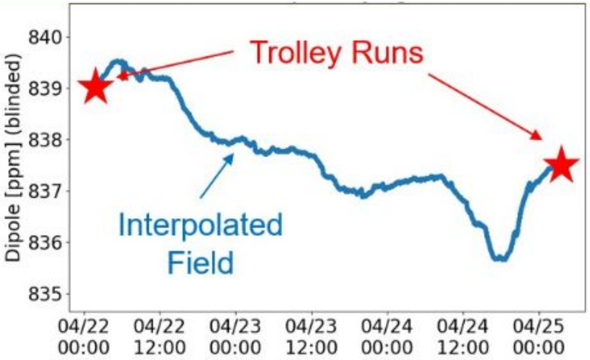

Measurement of the magnetic field, weighting with muon distribution map *M*

Muon distribution map and B-field map

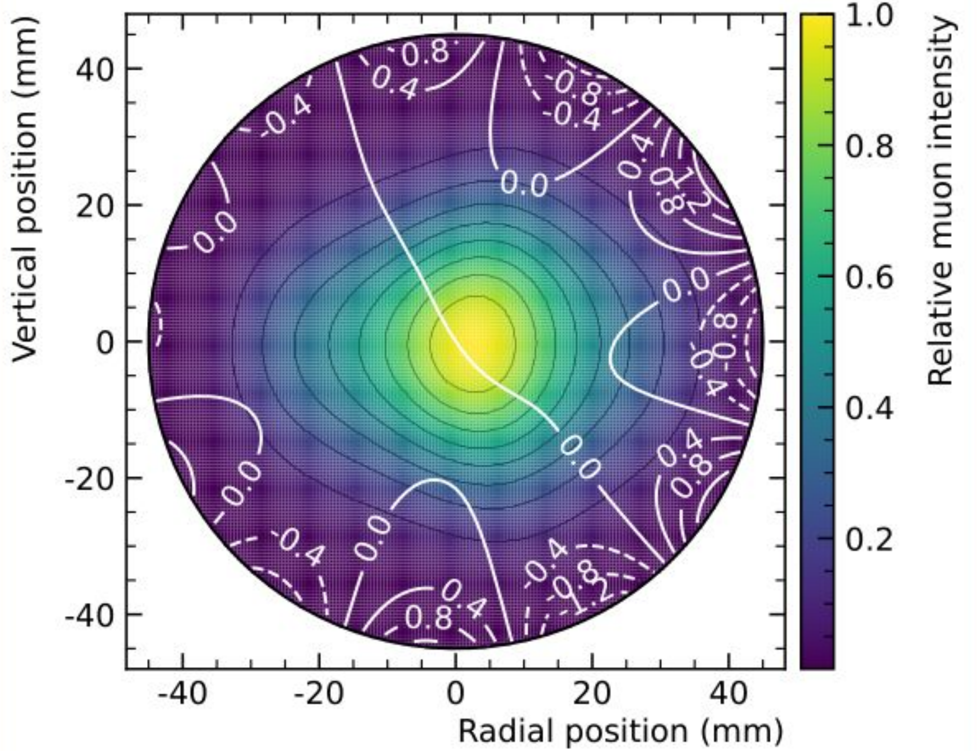

- Muon distribution map *M* reconstructed
- With trackers in close to trackers
- With trackers + simulation elsewhere

$\tilde{\omega}'_p(T_r)^m = \omega'_p(T_r)^m$ x *M B*-field map weighted with muon distribution map [48 ppb precision]

Corrections to $\omega_a{}^m$ and $\tilde{\omega}_p{}'(T_r)^m$

$$R'_\mu(T) = \overbrace{\omega_a}^{\text{corrected}} \Big/ \underbrace{\tilde{\omega}'_p(T_r)}_{\text{corrected}} = \frac{\overbrace{\omega_a^m}^{\text{measured}}}{\underbrace{\tilde{\omega}'_p(T_r)^m}_{\text{measured}}} \frac{1 + \overbrace{C_e + C_p + C_{pa} + C_{dd} + C_{ml}}^{\text{beam-dynamics corrections}}}{1 + \underbrace{B_k + B_q}_{\text{transient-fields corrections}}}$$

- C_e quadrupole electric field outside magic radius
- C_p (Pitch) spin-precession contribution from muon vertical oscillation motion
- C_{pa} (Phase Acceptance) time-variation of mean muon distribution phase from detector acceptance and beam motion
- C_{dd} (Differential Decay) time-variation of mean muon distribution phase from momentum-dependent muon lifetimes
- C_{ml} time-variation of mean muon distribution phase from momentum-dependent muon storage losses
- B_k transient B-field generated by kicker eddy currents
- B_q transient B-field from vibration of plates of pulsed electrostatic quadrupole field system

E-field correction C_e: largest one & largest systematic contribution

The largest correction: 347 ppb
Depends on radial muon distribution equivalent to momentum distribution obtained with three detectors:

- Calorimeters
  - Parasitic on data-taking
  - Measure injected muon bunches dephasing (how muons spread along the beam over time)
- improved elaborations

New on Run 4/5/6

- Trackers
  - Parasitic on data-taking
  - Complement with beam dynamics simulation
  - Measure muon radial distribution along ring
- Miniscifi (Minimally Intrusive Scintillating Fiber detector)
  - Dedicated runs
  - Complement with beam dynamics simulation
  - Measure muon radial distribution

New on Run 4/5/6

measured muon momentum distribution

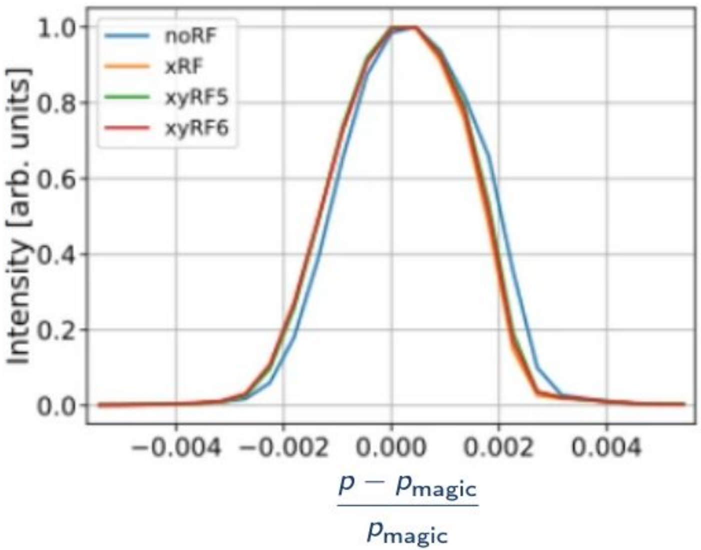

Miniscifi

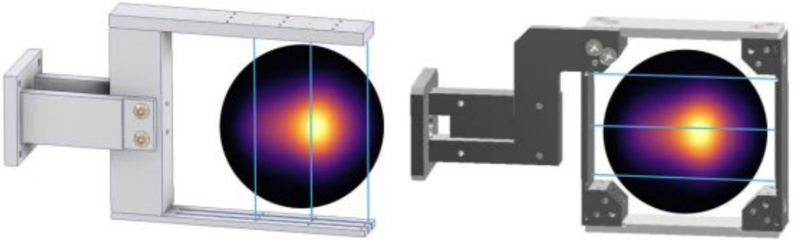

E-field correction C_e: largest one & largest systematic contribution

using 3 different consistent approaches ⇒ systematic uncertainty reduced to 27 ppb

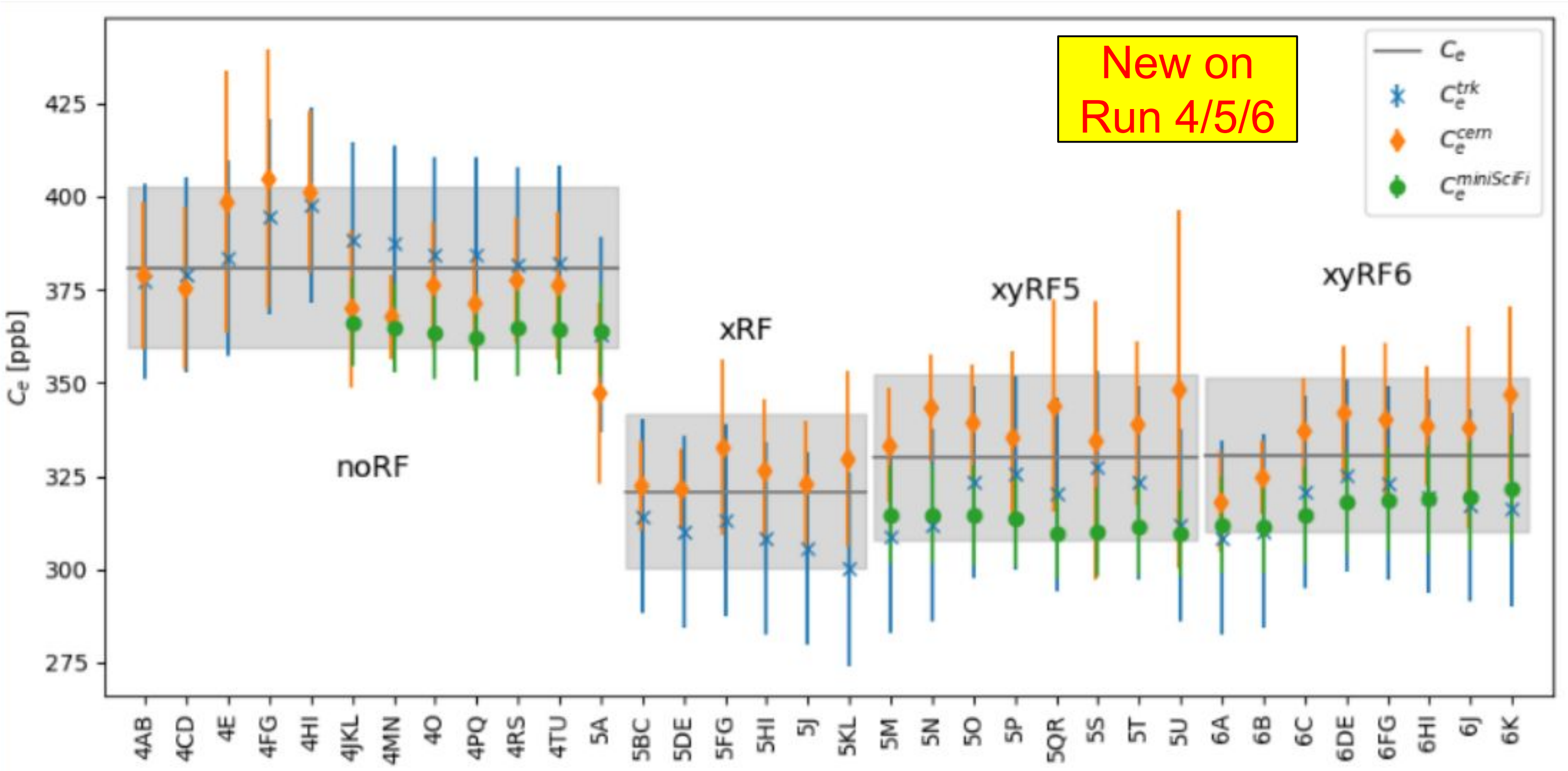

Kicker transient field measured with two magnetometers

New on Run 4/5/6

- Measure Faraday rotation of polarized laser light in TGG crystal
- Two independent teams and detectors
- Higher transient field measured off magic-radius
- Ckecks with hardware mockup
- −37 ± 22 ppb correction to B-field
- Run 1 & 2/3 results revised with improved understanding

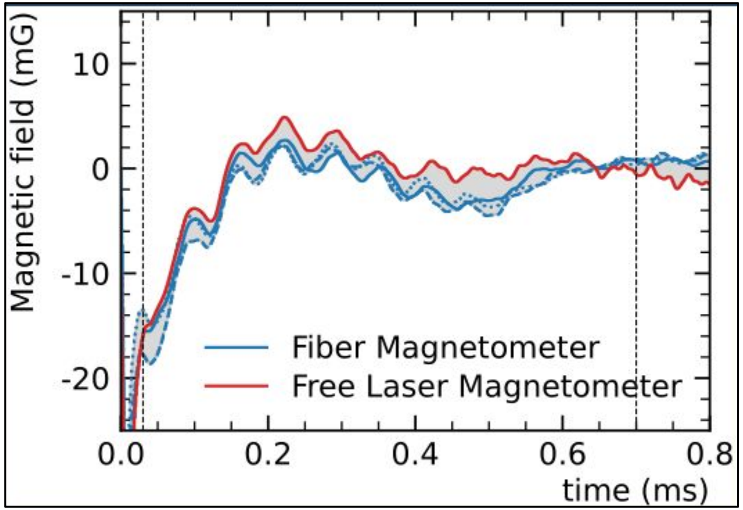

fiber magnetometer

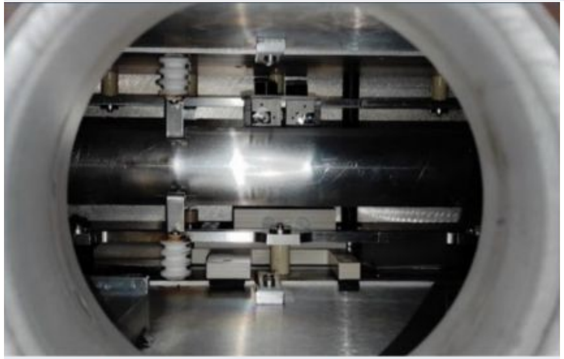

free laser magnetometer

Systematic corrections and uncertainties for Run 4/5/6

Quantity	Correction (ppb)	Uncertainty (ppb)
ω_a^m (statistical)	...	114
ω_a^m (systematic)	...	30
C_e	347	27
C_p	175	9
C_{pa}	-33	15
C_{dd}	26	27
C_{ml}	0	2
$\omega'_p(T_r)^m$ (mapping, tracking)	...	34
$\omega'_p(T_r)^m$ (calibration)	...	34
B_k	-37	22
B_q	-21	20
$\mu'_p(T_r)/\mu_B$	...	4
m_μ/m_e	...	22
Total systematic for $R'_\mu(T_r)$	**...**	**76**
Total for a_μ	**572**	**139**

$$a_\mu = \frac{\omega_a}{\tilde{\omega}'_p(T_r)} \frac{\mu'_p(T_r)}{\mu_B} \frac{m_\mu}{m_e}$$

- External inputs from CODATA 2022
- Tr = 25 °C

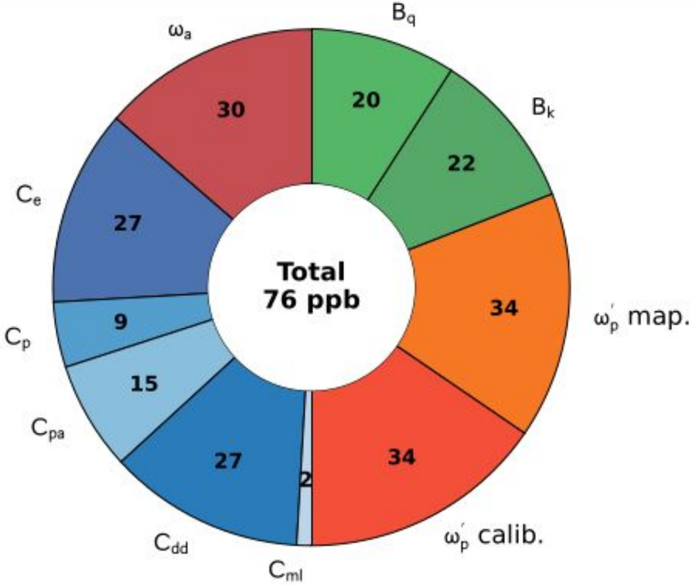

- Total systematic < 100 ppb (design)
- Systematics evenly distributed

Result

- Results blinded by unknown offset in calorimeter DAQ sampling frequency
- Collaboration approved result before unblinding on 20 May 2025
- BNL, FNAL Run 1 & 2/3 $R'_\mu(T_r)$, $\omega'_p(T_r)$ converted to spherical water sample at Tr = 25 °C
- FNAL Run 1 & 2/3 results revised
- Experimental results on $R'_\mu(Tr)$ have been combined (100% correlated systematics for FNAL measurements)
- PRL 135 (2025) 101802

Uncertainty

$R_\mu'(T_r)$	stat. [ppb]	syst. [ppb]	total [ppb]
Run-1	434	159*	462
Run-2/3	201	78*	216
Run-4/5/6	114	76	137
Run-1-6	98	78	125

*revised

23 ppb uncertainty from externally measured factors is not showed

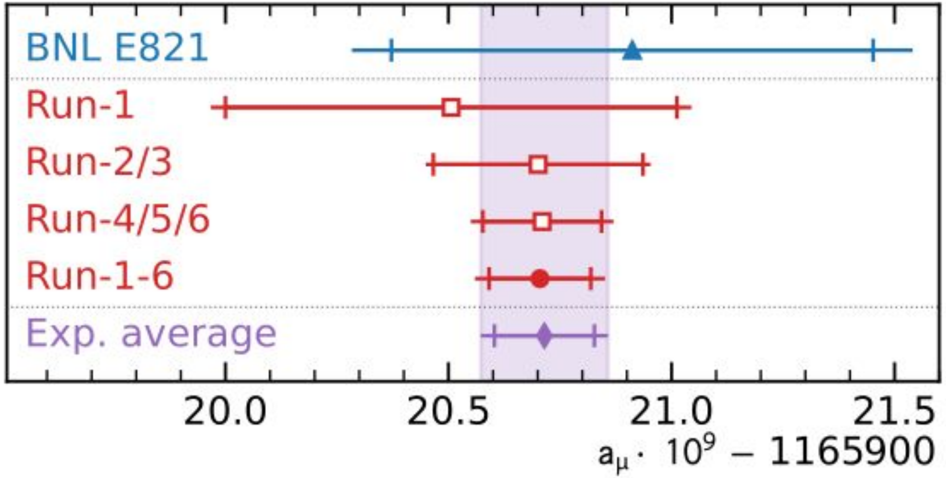

a_μ FNAL = 0.001165920705 (148) [127 ppb]
a_μ EXP = 0.001165920715 (145) [124 ppb]

Result

- Results blinded by unknown offset in calorimeter DAQ sampling frequency
- Collaboration approved result before unblinding on 20 May 2025
- BNL, FNAL Run 1 & 2/3 $R'_{\mu}(T_r)$, $\omega'_p(T_r)$ converted to spherical water sample at Tr = 25 °C
- FNAL Run 1 & 2/3 results revised
- Experimental results on $R'_{\mu}(Tr)$ have been combined (100% correlated systematics for FNAL measurements)
- [PRL 135 (2025) 101802](PRL 135 (2025) 101802)

Uncertainty

$R_{\mu}'(T_r)$	stat. [ppb]	syst. [ppb]	total [ppb]
Run-1	434	159*	462
Run-2/3	201	78*	216
Run-4/5/6	114	76	137
Run-1-6	98	78	125

*revised

23 ppb uncertainty from externally measured factors is not showed

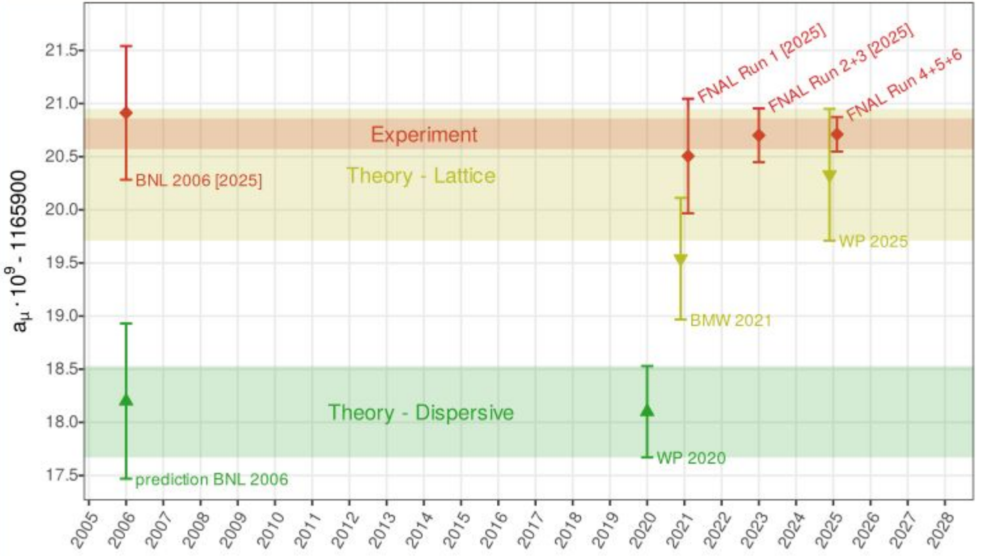

Conclusion

- Most precise a_μ measurement
- For many years to come
- Key ingredient of SM test
- Tight constraint on New Physics models

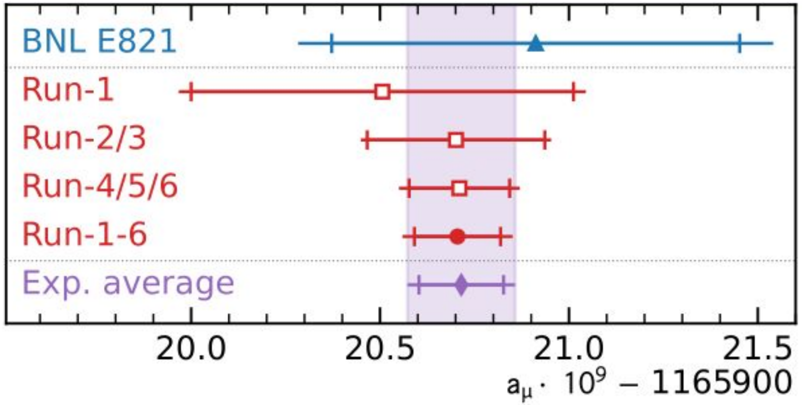

PRL 135 (2025) 101802

Acknowledgements

- Department of Energy (USA)
- National Science Foundation (USA)
- Istituto Nazionale di Fisica Nucleare (Italy)
- Science and Technology Facilities Council (UK)
- Royal Society (UK)
- Leverhulme Trust (UK)
- European Union's Horizon 2020
- Strong 2020 (EU)
- German Research Foundation (DFG)
- National Natural Science Foundation of China
- MSIP, NRF and IBS-R017-D1 (Republic of Korea)

Thanks!!

Backup

FNAL accelerator complex for Muon g −2

section of muon g-2 storage ring magnet

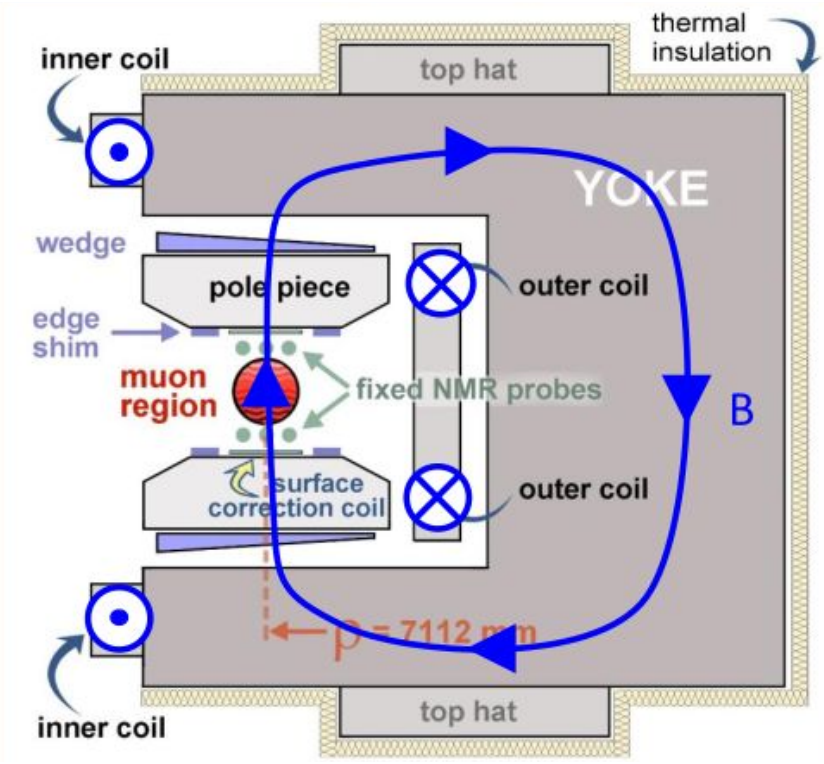

Pulsed inflector magnet injects muons into storage ring

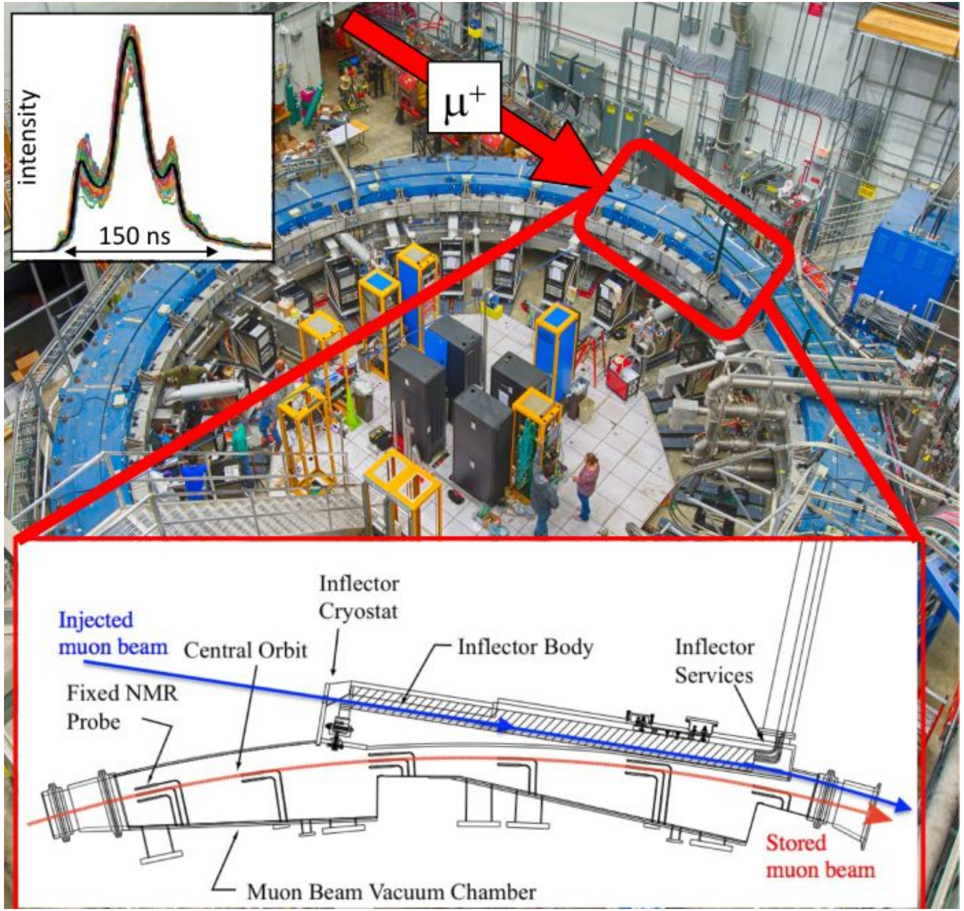

- Cancels 1.45 T field in beam channel
- Minimal perturbation of magnetic field in muon storage volume

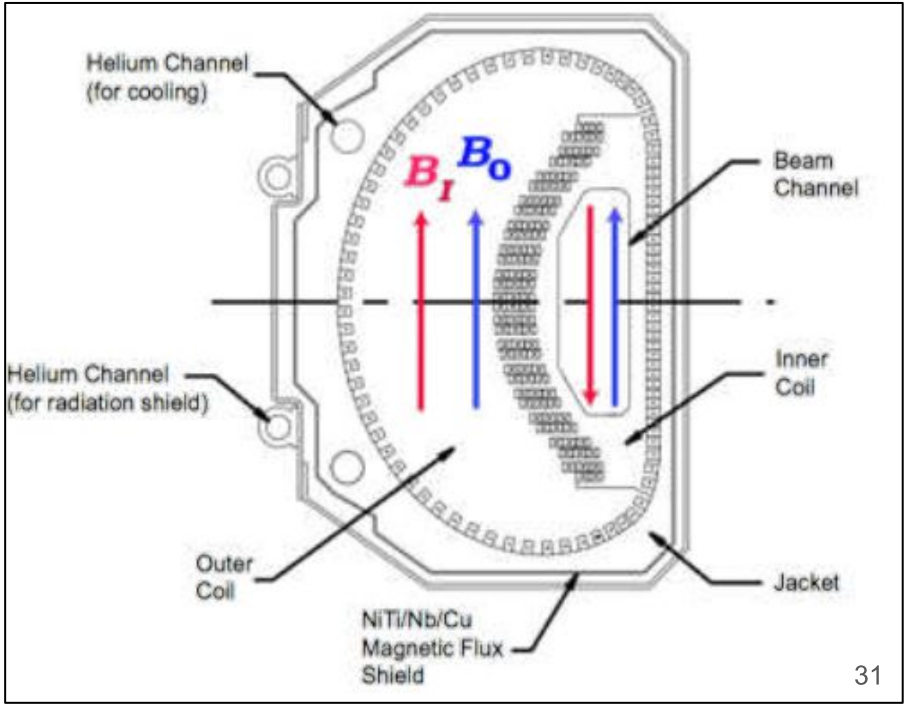

Magnetic kickers put muons into correct orbit

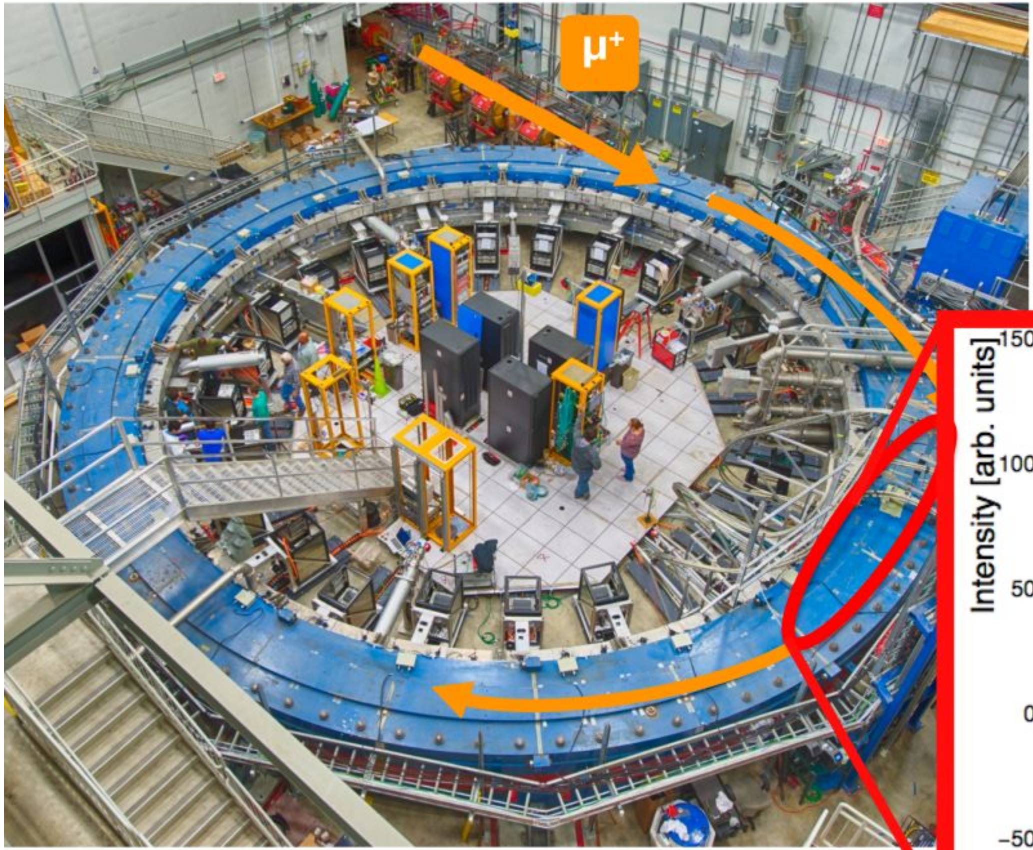

- 3 pulsed electro-magnets
- ~220 G magnetic field
- 3 − 4 kA peak current
- ~130 ns pulse duration, shorter than cyclotron period (149.2 ns)

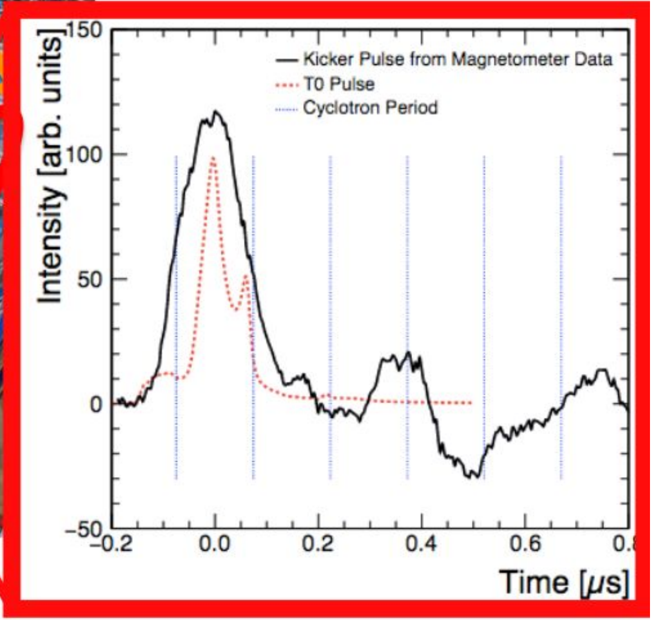

Electric quadrupoles focus beam vertically

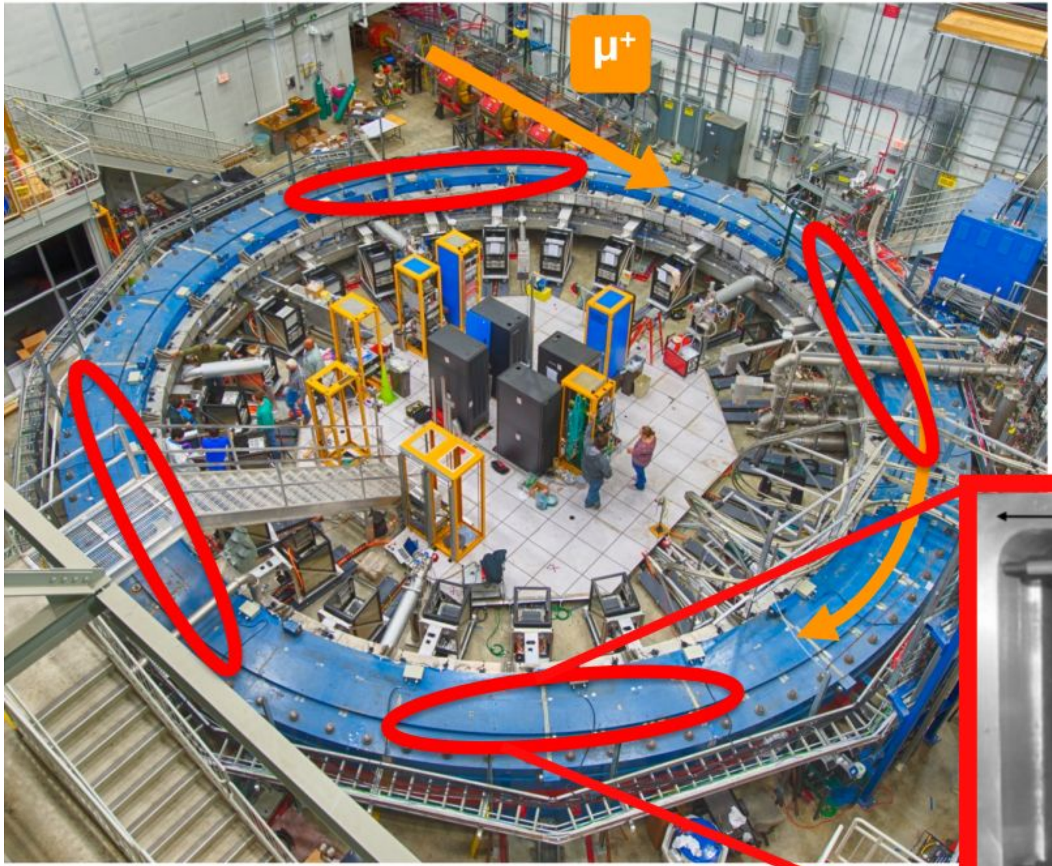

- Operated in ±15 − 21 kV range
- Pulsed to avoid spatial charge accumulation

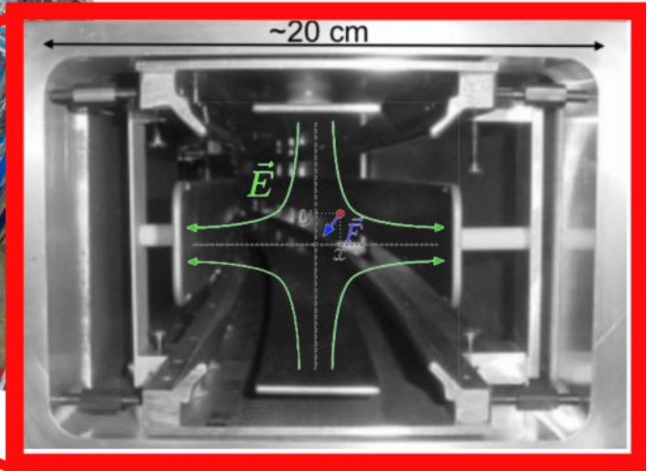

Measurement of the magnetic field, probes calibration

- Calibrate petroleum-jelly trolley probes with cylindrical H_2O probe (plunging probe) in same physical positions [20 ppb consistency and reproducibility]

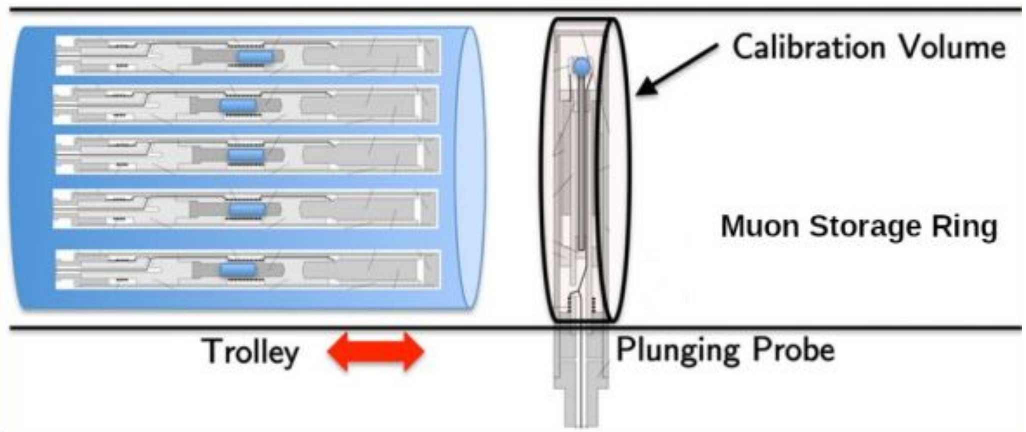

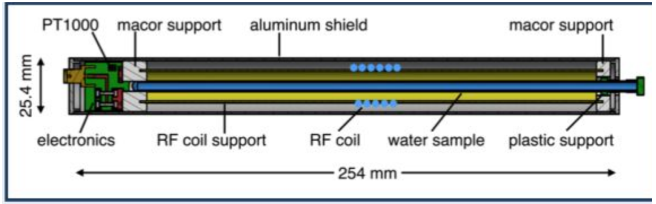

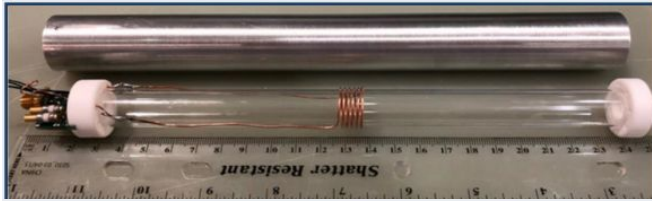

- Calibrate plunging probe in ANL MRI magnet
- Reference spherical H_2O probe [15 ppb precision]
- Reference 3 He probe [20 ppb precision]

H_2O probe

^3He probe

Run 4,5,6 ω_a measurements, 5 groups, 8 methods, 20 analyses

Groups (g)
BU
RE1
RE2
RE3
RE4
EU
Ky
SJTU

Reconstructions (r)
RW
RE
RI2
RQ

m	Measurement methods
T	Threshold
A	Asymmetry weighted
RT	Ratio T
RA	Ratio A
Q	Charge
RQ	Ratio Charge
ST	Stroboscopic T
SA	Stroboscopic A

rq	ratio quartering methods
R	random
K	kernel

Analyses			
g	m	r	rq
BU	T, A, RT, RA	RW	K
RE1	T, A	RE	R
RE2	T, A	RE	
RE3	RT, RA	RE	R
RE4	ST, SA	RE	
EU	T, A, RT, RA	RI2	R
UK	Q, RQ	RQ	R
SJTU	T, A	RW	

Pileup subtraction (ps)
RW-BU
RE
RW-EU
RW-SJTU

Envelope modeling
analytic function
spline
Gaussian Process Regression

Pulls – dealing with analysis-group-dependent blinding offsets

- I consistency checks for group-dependent blinding offsets possible relying on different datasets

- Pull = $$\frac{\left(\omega_a^{\text{dataset 2, analysis 2}} - \omega_a^{\text{dataset 2, analysis 1}}\right) - \left(\omega_a^{\text{dataset 1, analysis 2}} - \omega_a^{\text{dataset 1, analysis 1}}\right)}{\sqrt{\sigma^2\left(\omega_a^{\text{dataset 2, analysis 2}} - \omega_a^{\text{dataset 2, analysis 1}}\right) + \sigma^2\left(\omega_a^{\text{dataset 1, analysis 2}} - \omega_a^{\text{dataset 1, analysis 1}}\right)}}$$

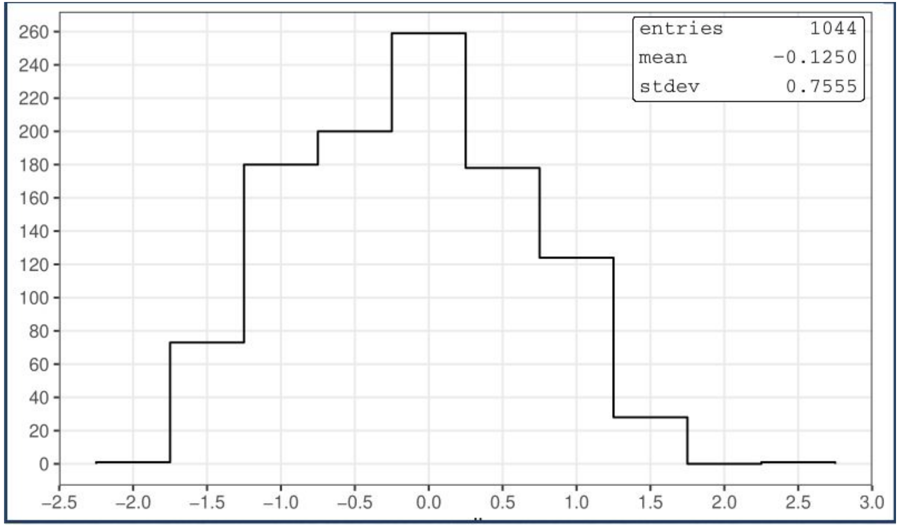

Pulls after removing group-dependent blinding offsets

$\omega_a{}^m$ measurements must be consistent within each dataset

20 $\omega_a{}^m$ measurements on 4 Run 4+5+6 datasets

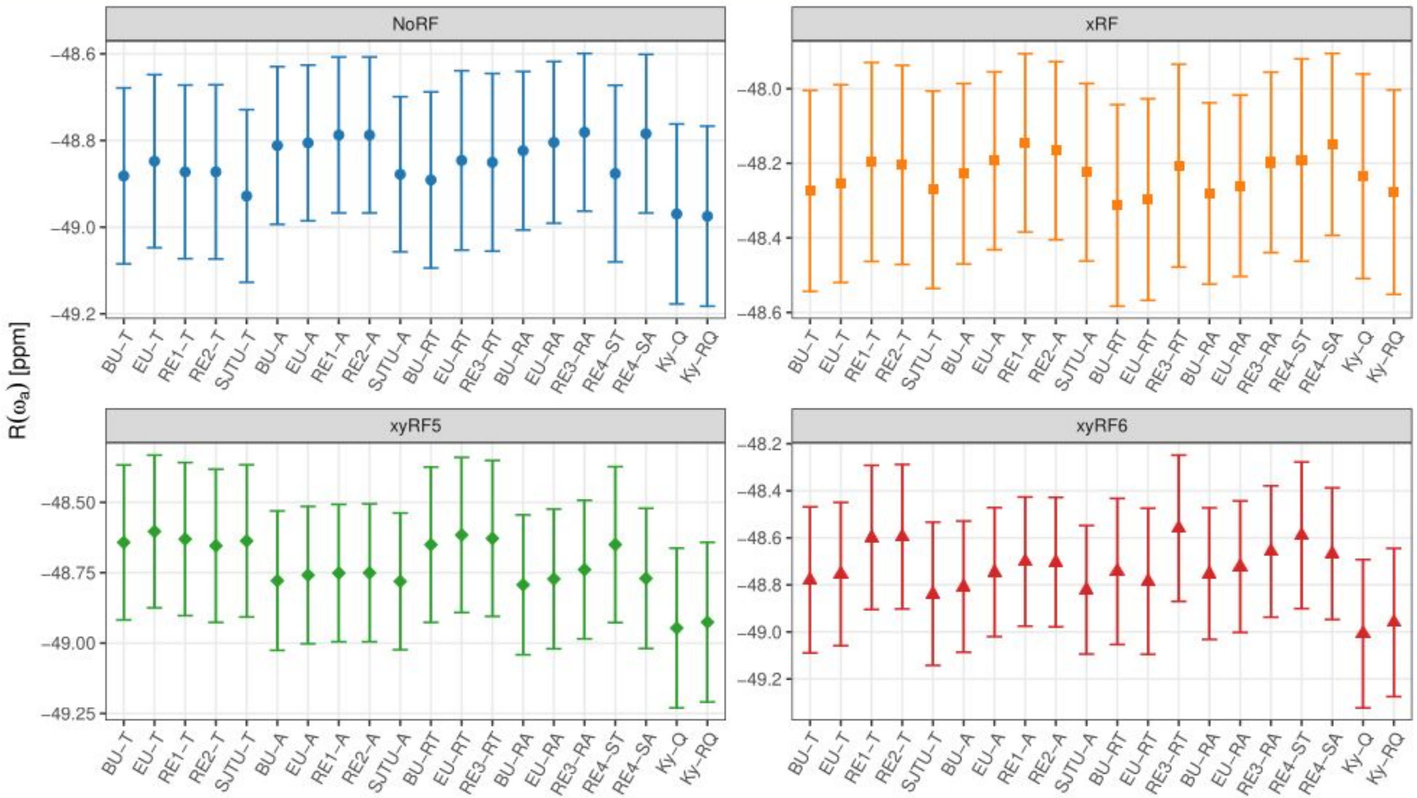

however, statistical uncertainties within same datasets are highly correlated

ω_a^m measurements with just their systematic uncertainties' estimates

20 ω_a^m measurements on 4 Run 4+5+6 datasets

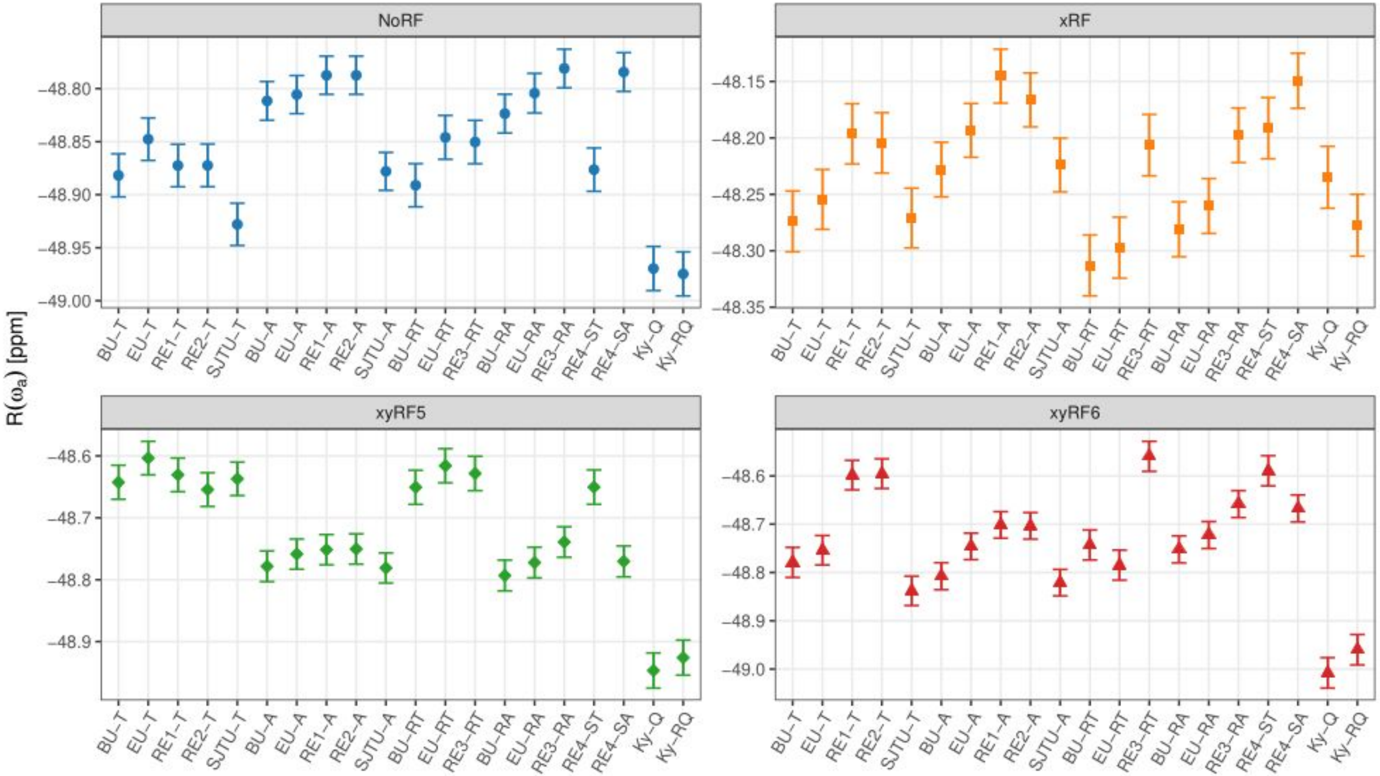

- Even assuming uncorrelated systematics, ω_a^m measurements are inconsistent
- Estimate variance-contributing statistical decorrelation between analyses using bootstrap samples

Consistency of Run 4/5/6 datasets, ω_a vs. $\tilde{\omega}'_p(T_r)$

Run 4+5+6 $R'_\mu(T) = \omega_a/\tilde{\omega}'_p(T)$ fit

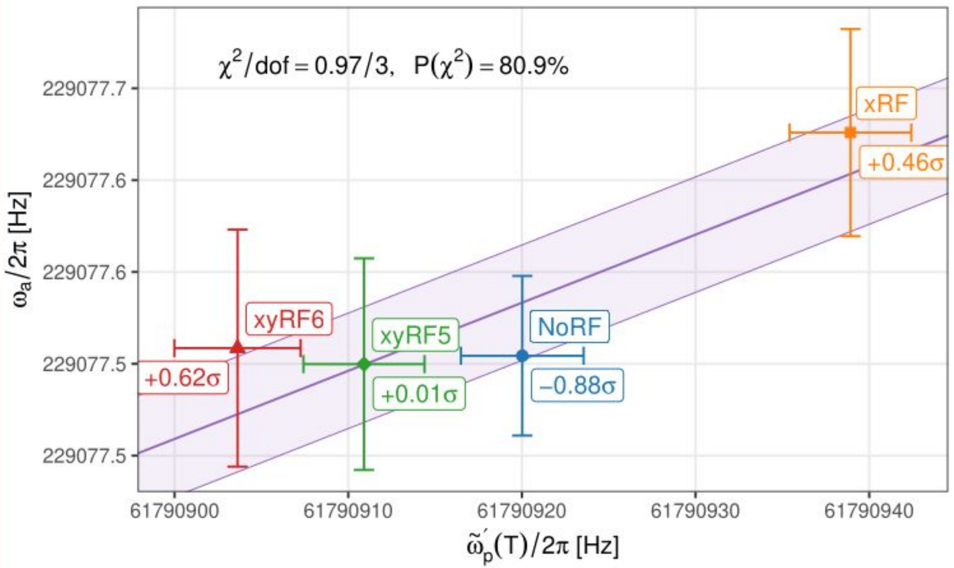

ΔR_μ measurements, common blinding

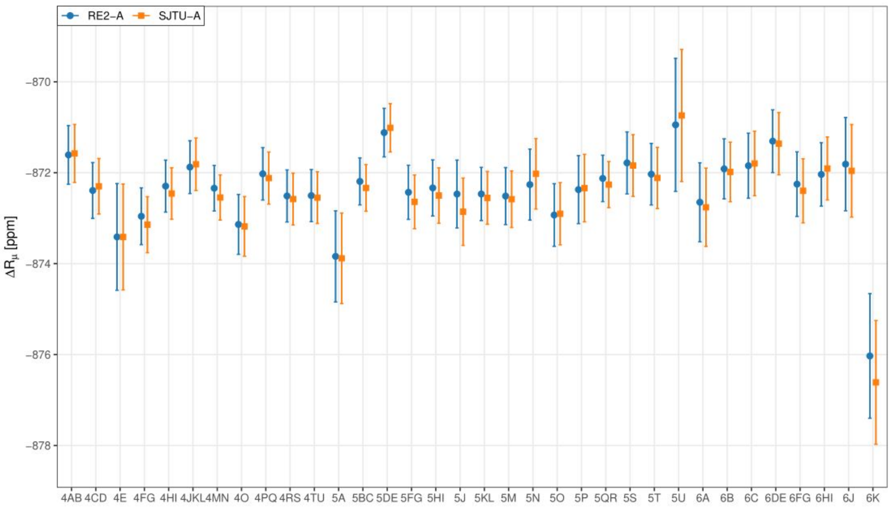

Consistency of BNL final report and FNAL datasets

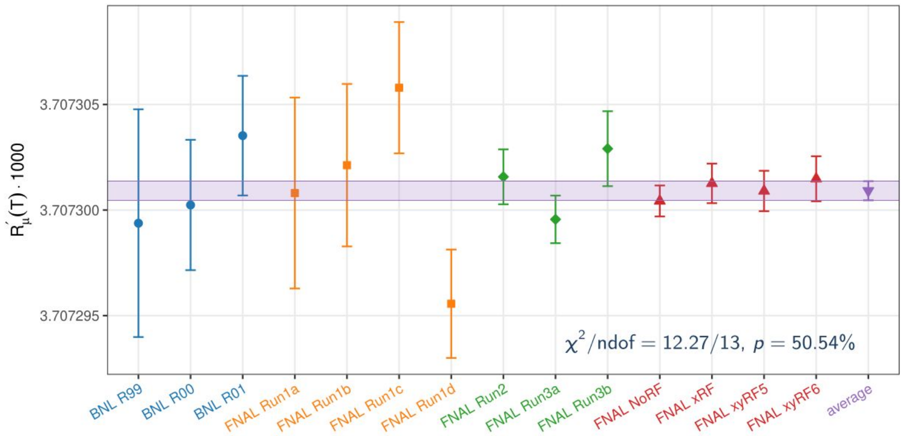

ω_a vs. $\tilde{\omega}'_p(T_r)$